# Correlated Charged Impurity Scattering in Graphene

Jun Yan and Michael S. Fuhrer*

*Center for Nanophysics and Advanced Materials and Materials Research Science and Engineering Center, University of Maryland, College Park, Maryland 20742, USA*

(Received 30 August 2011; published 7 November 2011)

We study electron transport properties of graphene in the presence of correlated charged impurities via adsorption and thermal annealing of potassium atoms. For the same density of charged scattering centers, the sample mobility sensitively depends on temperature which sets the correlation length between the scatterers. The data are well-understood by a recent theory that allows us to quantitatively extract the temperature dependence of the correlation length. Impurity correlations also offer a self-consistent explanation to the puzzling sublinear carrier-density dependence of conductivity commonly observed in monolayer graphene samples on substrates.

DOI: 10.1103/PhysRevLett.107.206601 PACS numbers: 72.80.Vp, 71.45.Gm, 81.05.ue

Understanding disorder in graphene [1] is essential for electronic applications; in contrast to conventional materials, the extraordinarily low electron-phonon scattering [2,3] in graphene implies that disorder [4–8] dominates its resistivity even at room temperature. Charged impurities [6,9–11] have been identified as an important disorder type in graphene on $SiO_2$ substrates [12,13], giving a nearly linear carrier-density-dependent conductivity $\sigma(n)$ and producing electron and hole puddles [14–16] which determine the magnitude of graphene's minimum conductivity $\sigma_{\min}$ [11]. Correlations of charged impurities are known to be essential in achieving the highest mobilities in remotely doped semiconductor heterostructures [17–19] and are present to some degree in any impurity system at finite temperature. Here, we show that even modest correlations in the position of charged impurities, realized by annealing potassium on graphene, can increase the mobility by more than a factor of 4. The results are well-understood theoretically [20], considering an impurity correlation length which is temperature-dependent but independent of impurity density. Impurity correlations also naturally explain the sublinear $\sigma(n)$ commonly observed in substrate-bound graphene devices [3,12,13,21].

Our experiment probes the influence of thermal annealing on the electronic transport properties of a graphene device with adsorbed potassium (K) atoms; potassium donates an electron to graphene, leaving a positive ion as a charged scattering center. We previously studied [22] charged impurity scattering in potassium on graphene at low temperature (20 K), where the K adatoms are presumed to be frozen randomly on graphene. Here, we measure the transport properties of graphene as the temperature is raised. We expect potassium ions on graphene to experience mutual Coulomb repulsion which drives them away from each other, producing correlations in their positions. Indeed, early low-energy electron diffraction studies of K adsorbed on graphite revealed a distinct diffraction peak, which is linked to the nearest-neighbor spacing of the dispersed K layer [23]. A recent scanning tunneling microscope study reached similar conclusions [24].

The graphene on the $SiO_2/Si$ sample was prepared by mechanical exfoliation of natural graphite (Nacional de Grafite Ltda.). Electrical contacts are defined with standard electron beam lithography and thermal evaporation of chromium and gold (5/90 nm). A photomicrograph of the device is shown in Fig. 1 (left inset). The sample is then annealed in $H_2/Ar$ gas at 350 °C for an hour before

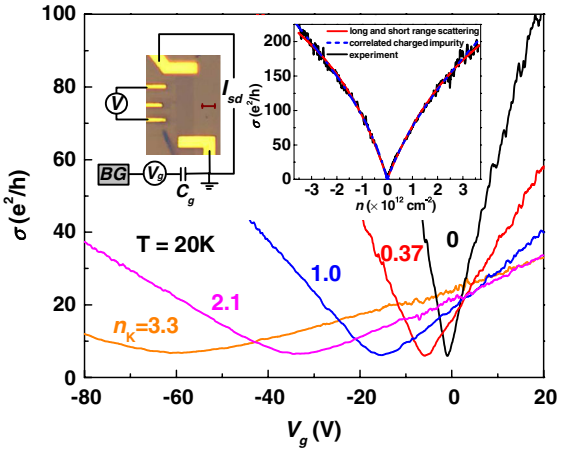


FIG. 1 (color online). Potassium deposition on graphene. The main panel shows the low-temperature (20 K) gate voltage dependence of the conductivity for the pristine device ($n_K = 0$) and successive depositions of potassium. The potassium density for each curve (see below in the inset of Fig. 3) is indicated (unit: $10^{12}$ cm$^{-2}$). The top-left inset shows an optical microscope image of the monolayer graphene device used in this experiment, with a schematic of the measurement circuit. The scale bar is 3 $\mu$m. The right inset shows the carrier-density-dependent conductivity of the pristine graphene device. The solid red curve is a fit to Eq. (1), and the dashed blue curve is a fit to the correlated charged impurity model (see text for fit parameters and discussion).

 

being mounted on a cold finger inside an ultrahigh vacuum chamber with a base pressure of $6 \times 10^{-10}$ Torr. We bake the sample at 200 °C under vacuum for a few days to further improve surface cleanliness. Figure 1 (right inset) shows the conductivity $\sigma$ of the pristine device after baking as a function of electron density $n = c_g(V_g - V_{g,\min})/e$, where $V_g$ is the gate voltage, $V_{g,\min}$ is the gate voltage of minimum conductivity, $c_g = 11$ nF/cm$^2$ is the gate capacitance, and $e$ is the elementary charge. The field effect mobility $\mu_{\rm FE} = \frac{1}{e}\frac{d\sigma}{dn}$ and Drude mobility $\mu_{\rm Drude} = \frac{1}{e}\frac{\sigma}{n}$ of the sample are about 20 000 cm$^2$/V s at a typical charge density of $10^{12}$ cm$^{-2}$, which are among the highest for graphene deposited on $SiO_2$/Si substrates [12]. Assuming Matthiessen's rule for long-range and short-range scatterers, the transport curve can be quantitatively described (solid red curve) by

$$\sigma_{\rm pristine}(n) = \left(\frac{1}{ne\mu_L} + \rho_S\right)^{-1} \quad (1)$$

(details of the fitting procedure are given in [25]). Equation (1) has been interpreted as reflecting scattering by uncorrelated charged impurities with $\mu_L = 26\,530(21\,700)$ cm$^2$/V s and by weak point disorder with $\rho_s = 53(55)\Omega$ for holes (electrons) [3,4,12,13,21], although no physical origin for the latter has been identified.

Potassium was deposited by electrically heating up a getter source (SAES Getters) with the sample kept at low temperature $T = 20$ K. Figure 1 (main panel) summarizes the effects of increasing potassium density on $\sigma(V_g)$ at $T = 20$ K. $V_{g,\min}$ shifts to increasingly negative gate voltages with increased potassium density, reflecting electron doping by potassium. The sample mobility decreases by more than an order of magnitude. These observations agree well with our previous studies [22].

We then measure $\sigma(n)$ at various temperatures from 20 to 180 K with a fixed $V_{g,\min}$ caused by potassium doping. This comprises one set of data with the same density of charged impurities while the impurity location and configuration are changed gradually by the rising temperature.

The K atoms are weakly bound to the graphene surface and desorb at high temperatures. Making use of this property, after completing one set of measurements, we bake the sample at 200 °C to remove K adsorbates. The sample becomes charge-neutral again, with mobility returning to the 20 000 cm$^2$/V s range. We then cool down to low temperature, and the experiment was repeated with a different K density. We observed no degradation of sample quality upon repeated experiments; after each baking prior to K doping, the sample mobility varied by ±10% and the $\sigma_{\min}$ occurred at gate voltages $-1$ V $\le V_{g,\min} \le 1$ V [25].

Figures 2(a)–2(c) show $\sigma(V_g)$ at different temperatures for potassium doping levels that result in $V_{g,\min}$ shifts $\Delta V_{g,\min} \approx 78$, 41, and 10 V, respectively. At all potassium

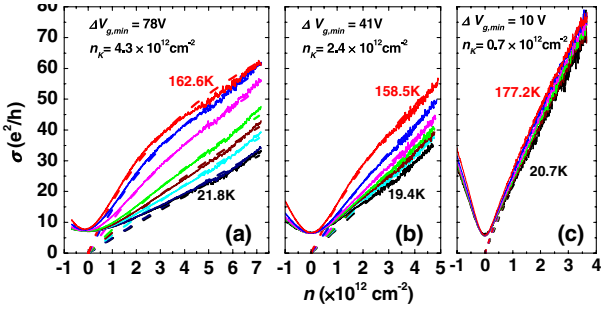


FIG. 2 (color online). Carrier-density dependence of graphene conductivity at various temperatures for three different potassium doping levels. (a) $\Delta V_{g,\min} = 78$ V. The temperatures are 21.8, 42.5, 100, 116.5, 130.1, 146.3, 156.6, and 162.6 K. (b) $\Delta V_{g,\min} = 41$ V. The temperatures are 19.4, 50.1, 94.9, 112.8, 126.8, 141.9, and 158.5 K. (c) $\Delta V_{g,\min} = 10$ V. The temperatures are 20.7, 132.7, 141.9, 150.4, 162, and 177.2 K. For each set, the curves are ordered from lowest to highest conductivity; the lowest and highest temperatures are also indicated in each panel. The dashed lines are fits to Eq. (3). The densities of potassium used as global fit parameters are shown for each panel.

doping levels, the conductivity increases with temperature, more rapidly for $T > 100$ K. The minimum conductivity point $V_{g,\min}$ remains fixed for $T < 180$ K, indicating that doping by potassium persists. (For $T > 180$ K, we observe $V_{g,\min}$ shifts toward 0 V, indicating potassium migration off the sample or desorption.) In addition to mobility improvements, $\sigma(V_g)$ also becomes significantly sublinear at elevated temperatures, in contrast to the linear $\sigma(V_g)$ expected [6,9–11,26] and observed [22,27] for isolated or clustered charged impurity scattering and observed here at $T = 20$ K. The mobility improvement and nonlinearity are most pronounced for the largest potassium doping (largest $\Delta V_{g,\min}$); the field effect mobility increases over fourfold for the largest $\Delta V_{g,\min}$.

In the Boltzmann formalism for charge transport, the square of screened Coulomb scattering potential $|\tilde{V}(q)|^2$ enters the relaxation time approximation when the charged impurities are uncorrelated. In the presence of correlation, estimation of relaxation time needs to take into account the structure factor $S(q)$ of the scattering centers and $|\tilde{V}(q)|^2$ is replaced with $|\tilde{V}(q)|^2 S(q)$ [28]. The structure factor is linked to the spatial distribution of potassium ions via a Fourier transformation. Here, we model the spatial correlation with a simple pair distribution function $g(r)$ recently proposed by Li *et al.* in Ref. [20]: $g(r)$ is 0 for $r < r_c$ and 1 for $r > r_c$, where $r_c$ is the correlation length, the single additional fit parameter. The corresponding structure factor is

$$S(q) = 1 - 2\pi n_{\rm K}\frac{r_c}{q}J_1(qr_c), \quad (2)$$

where $J_1$ is the Bessel function of the first kind and $n_{\rm K}$ is the potassium density. The resistivity $\rho_{\rm K}(n, n_{\rm K}, r_c)$ due to

scattering by correlated potassium ions may then be calculated by numerical integration [25].

Taking further into account the fact that there is some initial disorder in pristine graphene (right inset of Fig. 1) and that there exists temperature-dependent acoustic phonon scattering [2,29], we fit our transport curves with the following expression:

$$\sigma(n, n_K, T) = \{\sigma_{\text{pristine}}(n)^{-1} + \rho_{\text{ph}}(T) + \rho_K[n, n_K, r_c(T)]\}^{-1}. \quad (3)$$

$\sigma_{\text{pristine}}(n)$ is determined by fitting to Eq. (1) (see Fig. 1, right inset) and $\rho_{\text{ph}} = [0.1\ \Omega/\text{K}] \times T$. The only free fitting parameters in Eq. (3) are $n_K$ and $r_c$.

For each set of data, we treat $n_K$ as a global parameter while $r_c$ varies with temperature. We note that $r_c$ cannot be smaller than 4.9 Å, since the densest K overlayer on graphene is the close-packed $2 \times 2$ ($C_8K$) structure [23]. In our fits, we fix $r_c = 4.9$ Å at base temperature. With these considerations, we find that our data are well-described by Eq. (3), as shown by the dashed lines in Figs. 2(a)–2(c) (four additional data sets, as well as fits, are shown in [25]). The fits not only describe the mobility increase but also capture the increase in the curvature in $\sigma(n)$.

Figure 3 summarizes the fit parameters. The correlation length is found to increase monotonically with temperature and is insensitive to potassium density, which varies over an order of magnitude. The lack of variation of $r_c$ with

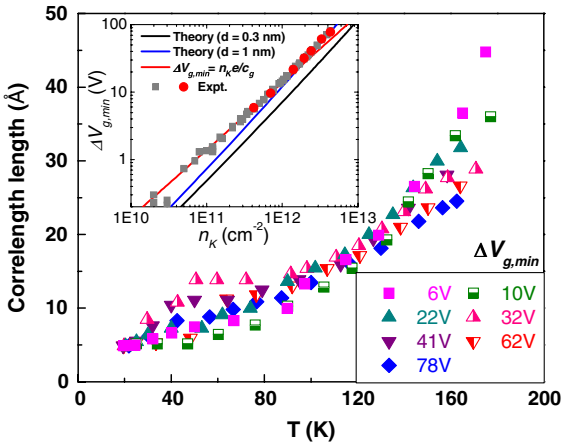


FIG. 3 (color online). Fit parameters for data in Fig. 2 to theory of correlated impurity scattering. The main panel shows the correlation length $r_c$ as a function of temperature for the seven sets of data at different potassium densities reflected in the shift of the minimum conductivity point $\Delta V_{g,\text{min}}$ indicated in the legend. The inset shows in log-log scale the $\Delta V_{g,\text{min}}$ dependence of the potassium densities $n_K$ obtained from the fits. The red circles correspond to the seven sets of temperature dependence data, and the grey squares are for other potassium doping levels measured at base temperature only. The lines are theoretical predictions discussed in the text [11].

density indicates that the short-ranged pairwise potential between potassium ions dominates the interaction and the hard-sphere repulsion model is appropriate. The correlation lengths found in Fig. 3 are smaller than the K-K distances $\pi n_K r_c^2 < 1$ even at the highest temperatures, consistent with this regime where the pair distribution model [20] is applicable. Using the convention that the close-packed $2 \times 2$ K overlayer corresponds to the coverage $\theta = 1$, the regime that is studied here is $0.001 < \theta < 0.01$. At similar K coverage, low-energy electron diffraction studies reveal that the K overlayer on graphite gives rise to a distinct diffraction peak that moves to higher wave vectors with adding of potassium and becomes better-defined at higher temperatures [30]. These observations are in accord with our experimental results, further substantiating our interpretation that correlation between potassium ions improves with temperature and strongly influences the transport properties of graphene devices. A recent study reported [24] strongly correlated potassium ($\pi n_K r_c^2 \approx 1$) deposited on graphite at 11 K at a density about twice the highest density studied here, probably reflecting a much more disordered landscape for potassium on highly corrugated [31] graphene on $SiO_2$.

The inset of Fig. 3 shows $n_K$ as a function of $\Delta V_{g,\text{min}}$. At low potassium densities $n_K < n_{\text{imp}} \sim 4 \times 10^{11}$ cm$^{-2}$, there is no theoretical prediction, but the simple prediction from geometric capacitance $n_K = \frac{C_g \Delta V_{g,\text{min}}}{e}$ describes our data well. At high potassium densities (greater than the initial impurity density $n_{\text{imp}} \sim 4 \times 10^{11}$ cm$^{-2}$; see below), the experimentally extracted $n_K$ vs $\Delta V_{g,\text{min}}$ can be described by the self-consistent theory for graphene in the presence of random charged impurity disorder [11,22] with the fitting parameter $d$ (distance of impurity to the graphene plane) equal to 1 nm. This deviation qualitatively indicates the incomplete screening by graphene predicted in [11]. That $d$ is somewhat larger than the expected potassium-graphene distance of 0.3 nm may indicate that the self-consistent approximation is not strictly quantitatively correct. Note that the temperature-dependent conductivity data used to probe correlations (Fig. 2) were taken at doping levels $n_K \geq n_{\text{imp}}$. For the highest doping levels, $n_K \approx 10 n_{\text{imp}}$, and it is reasonable to neglect $n_{\text{imp}}$ in our fits to the correlated impurity theory. That the theory also works well for $n_K \approx n_{\text{imp}}$ indicates that the single additional parameter ($r_c$) describes well the correlations of the mobile impurity population ($n_K$); however, we might expect $r_c$ to be different in the absence of the additional potential imposed by $n_{\text{imp}}$.

Figure 4 shows the temperature dependence of $\sigma_{\text{min}}$. $\sigma_{\text{min}}$ varies only slightly with potassium doping, as previously observed [22]. Within the self-consistent theory [11], $\sigma_{\text{min}} = n^* e \mu$, where $n^*$ is the residual (puddle) carrier density and $\mu$ the mobility. Interestingly, the temperature dependence of $\sigma_{\text{min}}$ is weak and is very similar to the undoped case ($\Delta V_{g,\text{min}} = 0$). This is surprising, given the

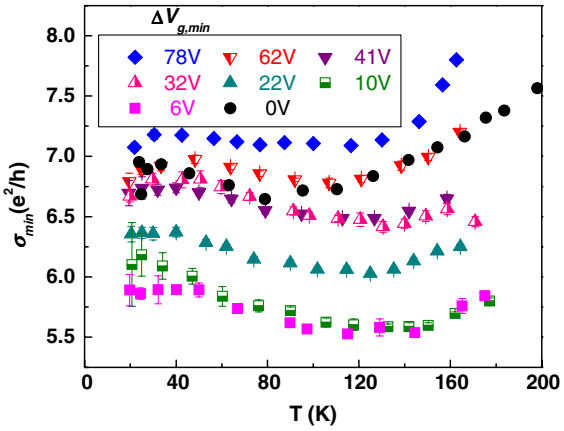


FIG. 4 (color online). Temperature dependence of the minimum conductivity. Black circles are for pristine graphene, and all other symbols are for various potassium densities given by the shift of minimum conductivity point $\Delta V_{g,\min}$ indicated in the legend.

large increase in mobility; it suggests a large decrease in the effective (puddle) carrier density at the minimum point for correlated disorder. More work is needed to understand this behavior.

The fact that impurity correlations always produce sublinear $\sigma(n)$ prompts us to revisit the interpretation of Eq. (1). While experimental evidence for long-range scattering ($\mu_L$) prevails [14–16,22], the source of the proposed weak short-range scattering ($\rho_s$) is mysterious. In particular, scanning tunneling microscope measurements have found that point defects in graphene lattice are extremely rare [15,16], and symmetry-breaking point defects are expected to give rise to resonant scattering [32], which experimentally gives a linear $\sigma(n)$ [7]. Meanwhile, it is quite likely that the long-range scatterers are correlated to some degree. We find that correlations in long-range scatterers alone can explain the observed sublinearity in $\sigma(n)$ without invoking point disorder.

In the right inset of Fig. 1, we refit $\sigma(n)$ for the pristine graphene sample to the theory for correlated charged impurities, and the result is shown as the dashed blue curve; fit parameters are impurity density $n_{\rm imp} = 4.6(3.9) \times 10^{11}$ cm$^{-2}$ and $r_c = 6.1(7.0)$ nm for electrons (holes). The fit is almost indistinguishable from Eq. (1). This is not surprising; for small argument of the Bessel function in Eq. (2), i.e., $\pi n r_c^2 \lesssim 1$, $\sigma(n)$ is well-approximated [20] by Eq. (1), with $\mu_L = \mu_0/(1-\alpha)$ and $\rho_s = 290\ \Omega \times \alpha^2$, where $\mu_0$ is the mobility for uncorrelated charged impurities, $\alpha = \pi n_{\rm imp} r_c^2 < 1$ [25]. This is consistent with the range of observed $\rho_s$ of 50–100 Ω on $SiO_2$ [3,13] and $h$-BN [21]. Charges are known to be mobile on the surface of $SiO_2$ on a time scale of seconds at room temperature [33]. Assuming that the $SiO_2$ mobile surface charges correspond to a nondegenerate plasma frozen at a temperature $T_0$ [17], the correlation length $r_c = \kappa k_B T_0/n_{\rm imp} e^2 \sim 6$ nm predicts $T_0 \sim 170$ K, which is a plausible temperature for freezing the trapped charge configuration of the oxide. More experiments are needed to understand the degree of correlation of disorder in various substrates used for graphene devices, but intentional correlation of disorder, e.g., by control of charge trap distributions or by rapid thermal annealing and quenching, should be a powerful tool to increase mobility in graphene devices.

We thank Qiuzi Li, E. H. Hwang, and S. Das Sarma for discussions. This work is supported by NSF Grant No. DMR 08-04976 and U.S. ONR MURI. The NSF UMD-MRSEC shared equipment facilities were used in this work.

*mfuhrer@umd.edu

[1] A. H. Castro Neto *et al.*, Rev. Mod. Phys. **81**, 109 (2009).
[2] J.-H. Chen, C. Jang, S. Xiao, M. Ishigami, and M. S. Fuhrer, Nature Nanotech. **3**, 206 (2008).
[3] S. V. Morozov *et al.*, Phys. Rev. Lett. **100**, 016602 (2008).
[4] N. H. Shon and T. Ando, J. Phys. Soc. Jpn. **67**, 2421 (1998).
[5] N. M. R. Peres, F. Guinea, and A. H. Castro Neto, Phys. Rev. B **73**, 125411 (2006).
[6] T. Ando, J. Phys. Soc. Jpn. **75**, 074716 (2006).
[7] J.-H. Chen, W. G. Cullen, C. Jang, M. S. Fuhrer, and E. D. Williams, Phys. Rev. Lett. **102**, 236805 (2009).
[8] J. P. Robinson, H. Schomerus, L. Oroszlány, and V. I. Falko, Phys. Rev. Lett. **101**, 196803 (2008).
[9] E. H. Hwang, S. Adam, and S. Das Sarma, Phys. Rev. Lett. **98**, 186806 (2007).
[10] K. Nomura and A. H. MacDonald, Phys. Rev. Lett. **98**, 076602 (2007).
[11] S. Adam, E. H. Hwang, V. M. Galitski, and S. Das Sarma, Proc. Natl. Acad. Sci. U.S.A. **104**, 18392 (2007).
[12] Y.-W. Tan *et al.*, Phys. Rev. Lett. **99**, 246803 (2007).
[13] C. Jang, S. Adam, J.-H. Chen, E. D. Williams, S. Das Sarma, and M. S. Fuhrer, Phys. Rev. Lett. **101**, 146805 (2008).
[14] J. Martin *et al.*, Nature Phys. **4**, 144 (2007).
[15] J. Xue *et al.*, Nature Mater. **10**, 282 (2011).
[16] Y. Zhang *et al.*, Nature Phys. **5**, 722 (2009).
[17] A. L. Efros, F. G. Pikus, and G. G. Samsonidze, Phys. Rev. B **41**, 8295 (1990).
[18] P. T. Coleridge, Phys. Rev. B **44**, 3793 (1991).
[19] E. Buks, M. Heiblum, and H. Shtrikman, Phys. Rev. B **49**, 14790 (1994).
[20] Q. Li, E. H. Hwang, E. Rossi, and S. Das Sarma, Phys. Rev. Lett. **107**, 156601 (2011).
[21] C. R. Dean *et al.*, Nature Nanotech. **5**, 722 (2010).
[22] J.-H. Chen *et al.*, Nature Phys. **4**, 377 (2008).
[23] Z. Y. Li, K. M. Hock, and R. E. Palmer, Phys. Rev. Lett. **67**, 1562 (1991).
[24] J. Renard, M. B. Lundeberg, J. A. Folk, and Y. Pennec, Phys. Rev. Lett. **106**, 156101 (2011).

[25] See Supplemental Material at http://link.aps.org/supplemental/10.1103/PhysRevLett.107.206601 for further discussion of sample preparation and measurement, details of the theory of correlated charged impurity scattering, data fitting procedure, and additional data sets.
[26] M. I. Katsnelson, F. Guinea, and A. K. Geim, Phys. Rev. B **79**, 195426 (2009).
[27] K. M. McCreary *et al.*, Phys. Rev. B **81**, 115453 (2010).
[28] G. D. Mahan, *Many-Particle Physics* (Plenum, New York, 1990).
[29] Polar optical phonons of the $SiO_2$ substrate may also contribute to the resistivity [2]. However, (1) for $T < 150$ K the polar optical phonon resistivity is negligible compared to the already small acoustic phonon contribution, and (2) $\sigma(n)$ for optical phonons is linear, so it would not produce the observed nonlinearity in $\sigma(n)$. We found that including optical phonon scattering changed the extracted $r_c$ values by less than 5%. See also [25] for a comparison of fits with and without optical phonon contributions.
[30] K. M. Hock and R. E. Palmer, Surf. Sci. **284**, 349 (1993).
[31] W. Cullen *et al.*, Phys. Rev. Lett. **105**, 215504 (2010).
[32] T. Stauber, N. M. R. Peres, and F. Guinea, Phys. Rev. B **76**, 205423 (2007).
[33] J. Lambert, G. de Loubens, C. Guthmann, M. Saint-Jean, and T. Melin, Phys. Rev. B **71**, 155418 (2005).